Irradiation Techniques: Synthesis of Polyaniline Nanocomposites for Use in Counter-Electrode Dyes in Solar Cells

Shawkat Salameh Gasaymeh*‡, Munir A. Elfarra**, Yasmin Mohamed Ibrahim ***, Youssef Taiser Laz****, Salem Silini*****

*‡ASD, Abu Dhabi Polytechnic, Abu Dhabi Polytechnic - Al Ain - Abu Dhabi - United Arab Emirate

** AET, Abu Dhabi Polytechnic, Abu Dhabi Polytechnic - Al Ain - Abu Dhabi - United Arab Emirate

*** The International Modern Arab School, The International Modern Arab School - Putra Jaya – Malaysia

**** ASD, Abu Dhabi Polytechnic, Abu Dhabi Polytechnic - Al Ain - Abu Dhabi - United Arab Emirate

***** High Institute of Science and Technology, High Institute of Science and Technology- Libya

(shawkat.gasaymeh@actvet.gov.ae, munir.elfarra@actvet.gov.ae, yasminabushady15@gmail.com, yousif.laz@actvet.gov.ae, salemomer19@gmail.com)

‡ Corresponding Author; Shawkat Salameh Gasaymeh, Abu Dhabi Polytechnic - Al Ain - Abu Dhabi - UAE,
Tel: +971501731969,
shawkat.gasaymeh@actvet.gov.ae

Received: 02.11.2023 Accepted:14.12.2023

Abstract- Due to the widespread acknowledgment of the need to transition towards eco-friendly energy and the stringent targets established for 2050, sustainable energy technologies are constantly evolving and taking on new forms. The solar cell is the most important of these new technologies. However, inefficiency and high production costs are still obstacles for solar cell technology when it comes to generating large-scale electricity. Within this paradigm, ongoing work is focused on increasing the efficiency of solar systems by incorporating nanotechnology and suitable materials. Conjugated polymers are fascinating because they can be designed at the molecular level to have tuneable energy gaps and electronegativity, allowing for the fabrication of conducting polymers with distinct ionization potentials and electron affinities. Polyaniline (PANI) is highly appreciated for its versatility in possible applications like solar cells, making it one of the most extensively investigated conjugated polymers. Although commercially unavailable, PANI can have its characteristics modified using molecular design and synthesis techniques. Dye-sensitized solar cells make extensive use of zinc sulfide/polyaniline (ZnS/PANI) nanocomposites due to their superior optical, electrical, catalytic, dispersibility, and agglomeration resistance. As an alternative to more expensive silicon-based solar cells, dye-sensitized solar cells (DSCs) show great promise. This article describes the one-step hybrid chemical irradiation method used to create (ZnS/PANI) nanocomposites. UV-Vis spectroscopy, transmission electron microscopy, and scanning electron microscopy were used to characterize the ZnS/PANI nanocomposite. The findings show that ZnS nanoparticles have robust interactions with polyaniline. The fundamental goal of this investigation is to learn more about ZnS/PANI nanocomposites as a promising new material for use in solar cells.

Keywords PANI, ZnS, flexible electronics, nanocomposites, solar cell.

1. Introduction

There are many researches regarding renewable energy and its applications in literature [1-4].

Research towards increasing the efficiency of solar cell technology has been spurred by the widespread acceptance of solar power as a reliable renewable energy option. When it comes to turning sunlight into energy, the counter-electrode in a solar cell is a crucial component. Scientists have been looking into new materials and synthesis techniques to improve the efficiency of counter-electrodes in dye-sensitized solar cells (DSSCs). Polyaniline (PANI) nanocomposites can be made utilizing irradiation procedures; these may improve the DSSCs' performance and durability [5]. Low efficiency and high production costs are two major shortcomings of conventional solar cells, which are caused by their reliance on silicon cells. This inefficiency results from the fact that solar photons need to have enough energy to jolt an electron out of a cell's band gap. When the energy of a photon is less than the energy of the band gap, the difference is dissipated as heat. As a result of these obstructions, solar cells lose about 70% of the incident sun energy [6].

There is hope that nanotechnology can improve solar cell efficiency, especially by lowering production costs. In an effort to reduce costs and boost energy production, photovoltaic cells based on conjugated polymers and their composites with metal nanoparticles and organic components are now under development [7]. Using nanotechnology to develop cheap solar cells would aid in environmental protection.

The great efficiency with which solar cells based on nanotechnology convert sunlight into usable energy makes them a leading contender for the future of Photovoltaics (PV) technology. Nanostructures with crystallite sizes comparable to carrier scattering lengths are responsible for this efficiency, as they significantly lower scattering rates and boost carrier collecting yields [8]. Because of their increased density of states, nanostructures also have a high absorption coefficient. These nanostructures can be made to absorb light of a particular wavelength by controlling their size. To realize these benefits outside of a cryogenic environment, however, has been difficult because of the high cost associated with producing periodic arrays of nanostructures with consistent diameters below 20 nm [9].

Interest in integrating inorganic nanoparticles into organic polymers has arisen due to the development of hybrid materials consisting of both organic and inorganic components. With improved optical, mechanical, magnetic, thermal, and optoelectronic capabilities, these nanocomposites find use in a wide range of technologies, including solar cells [10]. Polyaniline (PANI) is a conductive polymer that can be used as a solar cell counter-electrode due to its high electrical conductivity and high optical transparency. Scientists are aiming to improve its efficiency and stability by raising its conductivity and electrocatalytic activity [11].

Irradiation techniques provide a fast and green route to synthesizing PANI nanocomposites. In particular, gamma irradiation meets the need for environmentally friendly synthesis techniques because it is safe and produces no harmful by products [12]. In order to maximize the properties of nanocomposites, uniform dispersion of nanoparticles is essential, and this is where gamma irradiation comes in. In addition to being useful for counter-electrodes in dye-sensitized solar cells, it can increase the electrical conductivity of PANI and boost the catalytic activity of metal nanoparticles. Using this method, the nanoscale structure of PANI may be precisely manipulated, opening the door to the addition of a wide variety of nanomaterials that can further improve its capabilities [9].

In this study, we investigate the feasibility of utilizing irradiation methods for PANI nanocomposite synthesis in DSSCs. Our goal is to offer a thorough introduction to the processes involved in making these materials as well as a description of the methods used to characterize them and assess their performance. Our goal is to help solve the world's energy crisis by drawing attention to the potential and limitations of PANI nanocomposites in the field of solar energy conversion.

2. Methodology

The methodology consisted of two sections. Firstly, the materials used in this study to prepare the composites of ZnS/PANI include the supplier company's name. Secondly, the processes involved in preparing ZnS/PANI nanocomposites.

2.1. Materials

The samples were prepared using distilled and refrigerated supplies of dodecylbenzenesulfonic acid (DBSA, 98%, Aldrich), polyvinylpyrrolidone (PVP Mw = 10, Aldrich), and aniline monomer (Aniline, 99.8%, Aldrich). Aldrich's cadmium sulfate (ZnSO48H2O, 98%), ammonium sulfide ((NH4)2S5H2O), and ammonium persulfate (APS, 98%) were all used in their purified, unadulterated forms. Isopropyl alcohol (IPA) was used to sterilize all samples before the experiment, and deionized water was made in-house to exclude the possibility of radical contamination.

2.2. Preparation of Composites

A combined chemical/gamma irradiation approach was used to create ZnS/PANI/PVP core-shell nanocomposites. A homogenous solution (labeled A) was made by dissolving the necessary amounts of DBSA and PVP in deionized water and heating it to 70°C while stirring vigorously in a clean room. After the solution had cooled to room temperature, it was stored in the refrigerator and given a name.

Aniline and deionized water (labeled B) were combined in a separate procedure, swirled constantly for 30 minutes, and then placed in the fridge for subsequent use. ZnSO4 was dissolved in the appropriate amount of deionized water

(designated as C), and the resulting solution was agitated vigorously for 30 minutes before being stored in the refrigerator. After vigorously swirling APS in deionized water (designated D) for 30 minutes, the mixture was placed in the refrigerator to chill. Finally, after rapidly stirring a measured amount of ammonium sulfide in deionized water (labeled E) for 30 minutes, the mixture was placed in the fridge to chill. Refer to Table 1 for a breakdown of the steps involved.

Table 1. The process of manufacturing ZnS-PANI-PVP core-shell

THE FOLLOWING SOLUTIONS WERE PREPARED AS:	
First Step	[A]: DBSA + PVP + Deionized water heated (70 °C) under vigorous stirring (30 min) [B]: Aniline + Deionized water under vigorous stirring (30 min) [C]: ZnSO4 + Deionized water under vigorous stirring (30 min) [D]: APS + Deionized water under vigorous stirring (30 min) [E]: (NH4)2S.5H2O + Deionized water under vigorous stirring (30 min) [F]: 5 ml of IPA
Second Step	[A] + [B] under vigorous stirring (30 min) + [C] under vigorous stirring (20 min) + [D] Dropwise under vigorous stirring (15 min) + [E] Dropwise under vigorous stirring (15 min) + [F] Dropwise under vigorous stirring (5 min)
Then all samples were sealed and sent to gamma cell for irradiation at different gamma doses.	

Table 2. Illustrates the analytical methods used to generate our composites at different radiation levels (kGy)

Sample no.	DBSA (g)	Aniline (g)	APS (g)	$ZnSO_4$	$(NH_4)_2S$	γ- Dose (kGy)
1	4.5	1.5	2	1.5	0.4	10
2	4.5	1.5	2	1.5	0.4	20
3	4.5	1.5	2	1.5	0.4	30
4	4.5	1.6	2	1.5	0.4	40
5	4.5	1.5	2	1.5	0.4	50

Table 2 provides detailed information about the composition of all the samples. The samples were prepared by sequentially adding substances C, D, and then E, following a thorough mixing of A and B for 30 minutes to ensure a uniform solution. After a five-minute waiting period, IPA was added slowly to the mixture. The solutions were magnetically stirred for half an hour while nitrogen was bubbled through them. The resulting homogeneous, milky solution was exposed to varying levels of gamma radiation in a Gamma cell.

Each test tube contained five milliliters of IPA, two hundred milliliters of water, and 0.3 grams of PVP. Importantly, the molar ratio of aniline to APS remained consistent across all samples. This process yielded a green, translucent solution suitable for direct application on a wide range of surfaces. The Gamma cell utilized for irradiation was the GC-220 Excel type, employing 60Co gamma rays, with sample doses ranging from 10 to 50 kGy.

3. Results and Discussion

3.1. The Process of Forming ZnS/PANI

Gamma irradiation can impart stability to ZnS/PANI nanocomposites by reducing the chances of particle agglomeration and enhancing their resistance to environmental factors, such as oxidation and moisture. This increased stability contributes to the longevity and reliability of these materials in solar cell applications. It helps prevent the aggregation or agglomeration of metal nanoparticles within the PANI matrix. This ensures that the unique properties of individual nanoparticles are preserved and utilized effectively in the composite material. Gamma irradiation can be finely tuned by adjusting parameters such as radiation dose and exposure time. This allows researchers to tailor the properties of PANI nanocomposites to specific requirements, such as optimizing their electrical conductivity or catalytic activity for a particular application. Due to its scalability, this method can be employed for large-scale production of materials like solar cells. However, when it comes to producing monometallic or bimetallic nanoparticles, gamma irradiation-induced technology has emerged as a preferred choice. This is primarily due to its exceptional capability to produce entirely reduced and highly pure metallic nanoparticles, free from by-products and the need for reducing agents [8].

Nuclear radiation, being ionizing, generates positive ions, free electrons, free radicals, and excited molecules. Ionization takes place when an electron, previously confined in the outer orbital of an atom or molecule, acquires sufficient

energy from an irradiating particle to break free. During gamma-ray irradiation in colloidal solutions, metal ions can be reduced into zero-valent metal atoms by utilizing the solvated and ejected free electrons, all without the requirement for reducing agents or catalysts, which can trigger undesired side reactions [10].

In the process of polymerizing aniline into PANI, both the aniline monomer and $ZnSO_4$ become excited by photons. However, Zn^+ acts as an electron acceptor, simultaneously reducing Zn* and oxidizing the aniline monomer. Gamma irradiation supplies ample energy to interact with hydrated aqueous materials through photoelectric absorption, Compton scattering, and pair creation, resulting in the generation of secondary electrons through Compton scattering. These secondary electrons induce various reactions, including the creation of hydrated electrons (e^-_{aq}), as demonstrated in Equation (1).

The hydroxyl and hydrogen radicals (OH• and H•) formed in the radiolysis of water can be considered potent reducing agents in aqueous colloidal solutions, as indicated in Equation (2). These radicals initiate the decomposition and chemical reactions described further in a solution of $ZnSO_4$. As electrons are released, they combine with zinc ions Zn^+ to form zinc sulfide nanoparticles, or ZnS, in equations (3) and (4), it is evident that a substantial quantity of neutral zinc atoms (Zn^0) can be generated in the solution due to the high electron capture cross section for Zn^+ ions. Neutral Zn^0 atoms play a role in the formation of zinc nanoparticles in the solution by interacting with excess Zn^+ ions to create Zn^{2+} species, as shown in Equations (4).

$$nH_2O \xrightarrow{\gamma-raiation} e^-_{aq}, H^\bullet, OH^\bullet, H_2, H_3O^+, H_2O_2 \ldots etc \quad (1)$$

$$(NH_4)_2S + ZnSO_4 = ZnS + (NH_4)_2SO_4 \quad (2)$$

$$ZnSO_4 + (NH_4)_2S \xrightarrow{\gamma-raiation} ZnS + (NH_4)_4SO_4 \quad (3)$$

$$Zn^{2+} + SO_4^{2-} + ZNH_4^+ + S^{2-} \rightarrow ZnS + ZNH_4^+ + SO_4^{2-} \quad (4)$$

$$Zn^{2+} + S^{2-} \rightarrow ZnS \quad (5)$$

During the initial irradiation stage, aniline undergoes polymerization through the assistance of sulfate ions (SO3-) instead of zinc ions (Zn+). In this first phase, the aniline monomers are polymerized by the release of sulfate ions (SO3-) from zinc sulfate (⟦ZnSO⟧ _4) through photon breakdown. In the subsequent stage, zinc ions (Zn+) in the solution cause the oxidation of any remaining oligomers, dimers, or tetramers. This occurs because of the lower oxidation potential of zinc ions compared to the aniline monomers. As a result, increasing radiation doses and the DBSA doping method lead to the formation of ZnS/PANI core-shell composites through a competitive process involving oxidation and reduction. When aniline is exposed to gamma irradiation, the nitrogen atoms (N+) of aniline molecules become protonated by sulfate ions (SO3-), resulting in link scission, polymerization, and the formation of strongly protonated PANI. The reduction process induced by radiation-generated electrons causes the conversion of zinc ions (Zn+) into zinc sulfide (ZnS) nanoparticles, as previously explained for ZnS/PANI/PVP and illustrated in Figure 1.

Polymers can undergo radiation doping, but exposure to radiation can also induce chemical alterations in polymers, such as cross-linking, chain breakage, generation of C=C bonds, production of alkyne groups, and depletion of heteroatoms like N, S, or O. For more in-depth information, please refer to references [12].

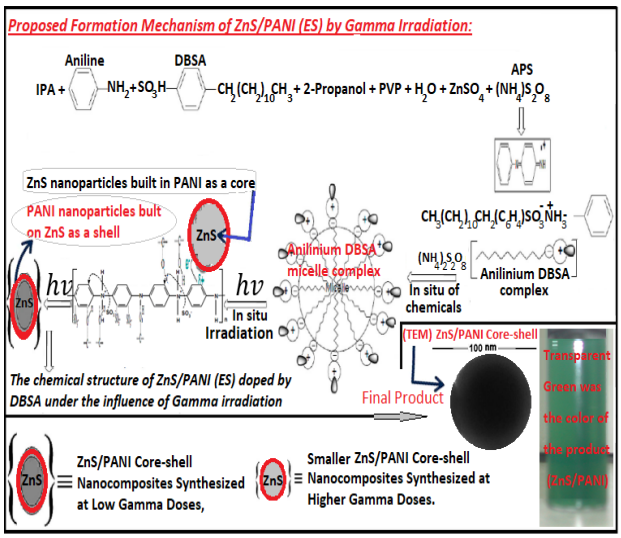


Fig. 1. A suggested explanation for the formation of ZnS/PANI involves the utilization of solid noble metal ZnS nanoparticles as the central core, with PANI nanoparticles enveloping them as the outer shell to form a core shell.

When polycarbonate is subjected to gamma rays, neutrons, ions, or electron beams, it is highly prone to chain breakage. Our research team has identified three distinct types of molecules in polycarbonate after treatment with heavy ions (specifically, 128 MeV Ar9+), as revealed through ultraviolet (UV) analysis [8]. The first type may form as a result of an intramolecular interaction involving phenoxy-phenyl and phenoxy-phenoxy radical pairs. The second type is a consequence of the radical's interaction with adjacent hydrogen, oxygen, or water molecules, leading to chain fractures and a subsequent reduction in molecular weight. These two categories may manifest at lower radiation doses. The third type emerges when molecules combine in a radical manner, typically occurring at very high doses. However, the substantial production of this third type of molecule offers the possibility of controlling the process. We anticipate a decrease in particle size due to polymer chain breakage, as evidenced by our scanning electron microscopy and conductivity experiments, which demonstrate increased conductivity and a narrowed energy band gap.

In this research, I delve into the previously mentioned doping approach in PANI composites, which entails a single process combining both gamma irradiation and DBSA acid doping methods. When irradiating PVP polymer at a low dosage, the higher binding energy of the C-C bond, as opposed to the C-H and C-OH bonds, makes it more likely to cause scission of C-H (with a binding energy of 4.37 eV) and certain C-OH side chain bonds [13]. The formation of new bonds like C=C and C=O in aldehyde compounds is expected to increase

with higher gamma irradiation doses [14]. As depicted in Figure 1, CdS/Polymer nanoparticles were created, resulting in a color shift from colorless at 0 kGy to green at lower doses and dark green at higher doses. This aligns with the predictions derived from the aforementioned equations and is consistent with prior findings related to PANI, Ag/PVP nanoparticles, and Ag/PANI core-shell nanocomposites [8].

3.2. Morphology and Particle Distribution

Scanning electron microscopy (SEM) results show that γ-irradiation and synthesis process have major effects on the morphology of ZnS/PANI. When subjected to gamma irradiation doses ranging from 10 to 50 kGy, changes in morphology can potentially take place due to a transformation in the polymer's structure. Exposure to radiation can induce diverse chemical transformations in polymers, encompassing cross-linking, chain breakage, and the formation of C=C bonds [15]. It has been reported that the nanocomposites of polyvinyl alcohol (PVA) and polyvinylpyrrolidone (PVP), polyaniline (PANI) have diameters between 100 and 150 nm [16]. These results suggest that the diameter of spherical nanoparticles can vary with the type of binder employed.

Uniformly sized and shaped ZnS quantum dots across the matrix remain challenging to manufacture. ZnS quantum dots, created by irradiation, could have a beneficial effect on particle size and dispersion if incorporated into polymer composites in this context. Figure 2 exhibits the ZnS/PANI composite, which was produced through a 40 kGy irradiation process. When we examined the SEM characteristics of PANI nanoparticles formed through irradiation at 30 kGy and compared them to those generated at 40 and 50 kGy, we identified that the diameter of the spherical nanoparticles in ZnS/PANI core-shell nanocomposites was approximately 100 nm (as shown in Figures 2 and 3).

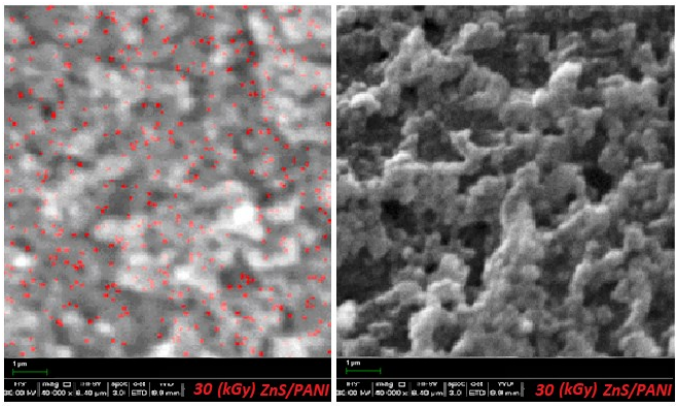


Fig. 2. SEM of ZnS/PANI nanocomposites with a core-shell structure synthesized through irradiation at 30 kGy.

In a previous study, we reported similar observations in the case of Ag/Polyaniline, indicating that the presence of ZnS has a minimal to negligible influence on the PANI morphology. Figure 3 displays an image illustrating the surface structure of ZnS/Polyaniline core-shell nanocomposites created through 50 kGy irradiation. These were notably smaller (around 20 nm) in comparison to ZnS/PANI core-shell nanocomposites formed through 30 kGy irradiation (measuring 100 nm). ZnS quantum dots were formed at the core of PANI nanoparticles, and scanning electron microscopy images suggest that these particles adopt a core-shell configuration. The structure of ZnS/PANI core-shell nanocomposites produced at 30 kGy is observable in SEM micrographs, which is why the impact of gamma irradiation on shape requires further investigation. Despite an increase in size to approximately 400 nm when compared to those created at a higher irradiation dose, the results demonstrate the preservation of particle morphologies.

Scanning electron micrographs were used to perform element mapping on ZnS/Polyaniline core-shell made at 30 kGy (Figure 2). This finding demonstrates the number and distribution of Zn-S (sulfur) within the nanoparticles, providing further evidence for the production of ZnS quantum dots PANI. ZnS quantum dot sizes cannot be discerned from SEM micrographs. For ZnS/PANI core-shell nanocomposites, the morphological information provided by SEM research is limited. In Figure 2, the Zn is shown as red dots. If confirmed, this result would lend credence to the theory that ZnS can be formed by γ-irradiation techniques.

Based on SEM morphological analysis, we found in a prior study by Gasaymeh and Almansoori [17] that the PANI nanoparticles formed in Ag/PANI nanocomposites have a diameter of 50–100 nm. We found Ag nanoparticles within the polymer in nanosized with a mean radius of about 10 nm using transmission electron microscopy. The core of a PANI nanoparticle is an Ag nanoparticle. Our hypothesis was that the Ag and PANI nanoparticles in the Ag/PANI nanocomposites were held together through a combination of hydrogen bonding and electrostatic interactions with the stabilizers. Anyhow, as seen in Figure 4, the EDX peaks of ZnS produced at different concentrations are of variable intensities. It's possible that a higher proportion of ZnS is formed from ZnSO4 as a result of the higher dose.

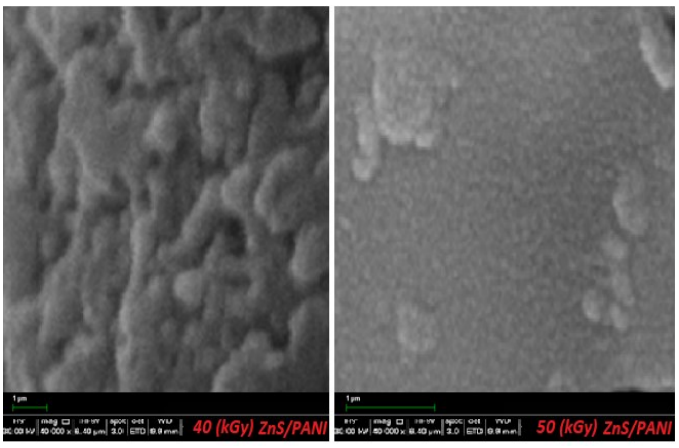


Fig. 3. SEM of ZnS/PANI nanocomposites with a core-shell structure synthesized through irradiation at 40 and 50-kGy.

Prior research conducted by our laboratory indicates that subjecting conducting PANI nanoparticles and modified PANI composites (Ag/PANI and CdS/PANI) with gamma radiation leads to a reduction in particle size and enhances their dispersion. Subsequent SEM images captured seven months after exposing ZnS/PANI core-shell nanocomposites,

produced with a 50 kGy dose, to atmospheric conditions, reveal their remarkable resilience to environmental factors. The utilization of gamma irradiation for the synthesis of metal nanoparticles has a multitude of practical applications. The deprotonation of metal ions, facilitated by hydrated electrons generated through gamma irradiation, ultimately results in the formation of neutral metal atoms [17]. These elementary particles, which can be as small as a single zinc atom, eventually cluster together to create larger structures.

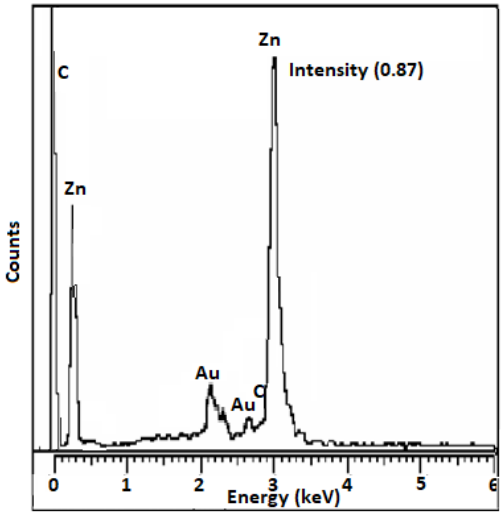


Fig. 4. EDX of ZnS quantum dots in ZnS/Polyaniline produced at 40-kGy.

The presence of ZnS nanoparticles in the red precipitate generated following gamma irradiation of a mixture consisting of DBSA, PVP, aniline, and ZnSO4 was further confirmed through scanning electron microscopy. After subjecting the mixture to gamma irradiation, PANI and ZnS nanoparticles developed concurrently, as evidenced by scanning electron micrographs of the precipitate. Additionally, the hydrophobic nature of PANI and the presence of protonated amine or imine sites deterred ZnS nanoparticles from adhering to the PANI surface [17]. This leads us to hypothesize that ZnS nanoparticles preferentially adsorb onto or embed within PANI. The absence of substantial aggregation of ZnS nanoparticles within PVP/PANI may be attributed to electrostatic interactions between PANI sites and ZnS atoms [18].

3.3. The TEM Analyses of Modified PANI (ZnS/PANI) Core-shell Nanocomposites

The results were obtained using a transmission electron microscope (TEM). To achieve this, a solution containing composite powder was placed on a copper grid and dried before TEM examination. Various TEM images were taken of ZnS/PANI/PVP quantum dot core-shell structures at different irradiation doses to investigate how these doses affected the conversion of ZnSO4 into ZnS quantum dots within PANI.

With higher doses of irradiation, ZnSO4 was converted into ZnS quantum dots, PANI ES was formed from its aniline monomer in PVP, and smaller particles with increased dispersion were observed. PVP, while acting as a binder in the composites, also prevented the formation of large ZnS quantum dot aggregates, ultimately limiting the size of the produced quantum dots and nanoparticles similar result was obtained by our research group [18]. In this study, the hydrophilic properties of PVP were utilized to protect the surfaces of the ZnS quantum dots.

The spherical ZnS nanoparticles in the TEM images appeared unaffected by the PANI applied to their surfaces. Within the core, a variety of ZnS quantum dot nanoparticles in different shapes and sizes predominated, while the outer shell was composed of PANI with varying thicknesses, depending on different parameters. ZnS/PANI core-shell nanocomposites (Figure 5) were created under the same conditions but with varying irradiation doses, as evidenced by TEM images. The radiation caused the size of CdS particles to decrease, going from over 400 nm at 10 kGy to 200 nm at 20 kGy, 90 nm at 30 Gy, and less than 10 nm at 50 kGy.

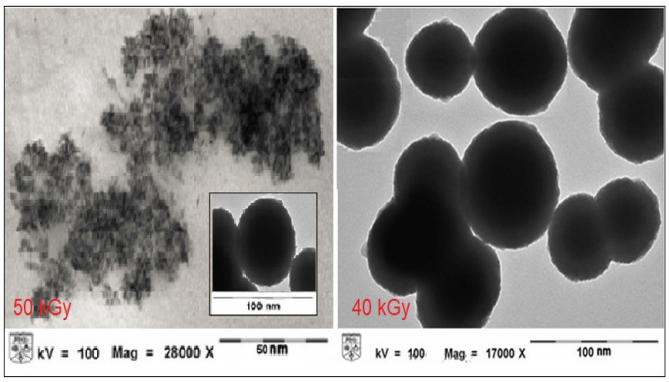


Fig. 5. TEM microscope images of ZnS/Polyaniline produced at radiation doses of 40 kGy and 50 kGy.

In addition, TEM images show how ZnS quantum dots are dispersed throughout PANI nano-spheres, providing further evidence that our goals have been attained and that PANI nano-spheres uniformly absorb ZnS quantum dots as a core and PANI as shell. However, the average size of ZnS quantum dots nanoparticles can be calculated. The absence of secondary aggregation of ZnS provides support for this discovery. Potential factors contributing to the size variations include a greater ZnSO4 to aniline molar ratio, the impact of aniline capping on ZnS quantum dots, and the integration of aniline molecules onto the surface of ZnS nanoparticles. Modifying the molar ratio of CdSO4 to aniline in Ag/PANI core-shell nanocomposites yielded outcomes similar to what we previously reported in our published work [17].

As a result of the polymerization, the ZnS quantum dots appear to have served as nucleation sites, resulting in a continuous PANI shell around them which support our proposed formation mechanism. It was shown that polyaniline nanocomposites (PANI) doped with 19 wt% aniline and 50 kGy have a spherical form. In the polymerization process, partially stabilized aniline molecules serve as caps, which may explain why nanoparticles with an aniline to ZnS weight ratio of less than 16 wt% have a unique size and form. Changes in particle size and form may, however, be attributable to the decreased aniline capping over ZnS quantum dots and the likely use of aniline molecules on the particles' surfaces. It appears that during polymerization, the smaller nanoparticles

of ZnS quantum dots merged into larger ones due to the lower capping of the stabilizer.

3.4. UV-VIS. Spectra of ZnS/PANI Core-shell Nanocomposites

While studying their optical characteristics with UV-vis spectroscopy, researchers found that the absorbance at the 800 nm band for conducting PANI increased exponentially with the increase in γ-dose (kGy) or/and with the addition of DBSA. ZnS/PANI core-shell nanocomposites dispersed in PVP at varying Gamma irradiation doses are shown in their UV-visible absorption spectra in Figure 6. In the conducting ES state of PANI in water, three characteristic absorption bands appear at 350, 420, and 800 nm due to the radical cation (polaron) state generated on the PANI backbone chain [17]. The polaron band transition is linked to the absorption band observed in the 430-450 nm and 790-810 nm ranges, as demonstrated by our work with ZnS/PANI core-shell nanocomposites. The addition of ZnS nanoparticles in the composites causes a shift in the peak around the 420 nm to higher bands, which may be related to doping and correlate to localization of electrons, as compared to pure PANI nanoparticles and Ag/PANI, published by our research group [17]. The absorption band shift is due to the overlap in ZnS absorption at 420 nm [5]. As mentioned in [17], our research group found analogous outcomes for Ag/PANI core-shell and pure PANI nanoparticles. In the instance of ZnS/PANI nanocomposite, the UV absorption bands at 345 nm can be attributed to the π ← π* transition on the PANI backbone.

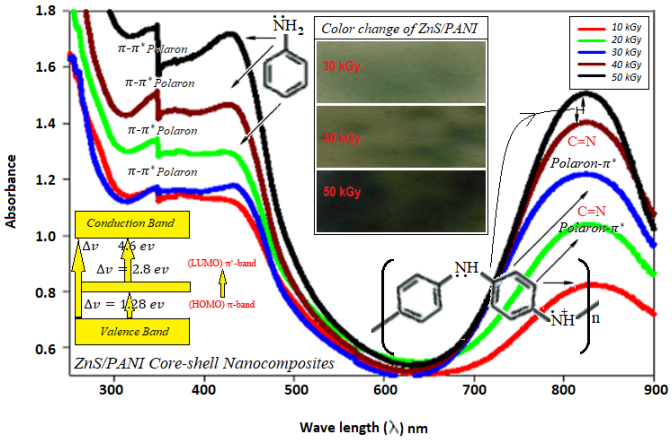


Fig. 6. The UV-vis absorption spectra of ZnS/Polyaniline.

While we didn't achieve the 830 nm wavelength observed in pure PANI nanoparticles [19], the presence of bands around 800 nm in all these spectra strongly indicates the protonation of PANI in ZnS/PANI core-shell nanocomposites. The electronic spectra of ZnS/PANI core-shell nanocomposites show both the π ← π* transition and the polaron transition, albeit at slightly different wavelengths depending on the specific parameters (dopants) involved. As there's no evidence for the electronic absorption of fully oxidized pernigraniline, which is expected at 600 nm and 320 nm [17], it's confirmed that the oxidation state of the synthesized ZnS/PANI core-shell nanocomposites in this study corresponds to their ES form, which is the conductive state of PANI within the ZnS/PANI core-shell structure.

Due to structural changes brought about by the insertion of Zn ions, PANI gradually narrows this band from a highly conductive emeraldine (ES) to a less conductive emeraldine [20]. A similar effect occurs when other dopants are introduced to PANI [21]. The increased competition from additional counter ions favors the compact coil structure of PANI at higher ZnSO4 concentrations. The 800 nm band becomes more prominent as the kGy, DBSA concentration, and aniline concentration increase. Enhanced conductivity and a higher degree of polymerization completion are both indicative of an increase in absorbance. Our earlier research in [17] yielded similar results with both pure PANI and Ag/PANI. Absorbance, or wavelength, increases with radiation dose since high-energy photons are converted into the kinetic energy of bound electrons in an atomic or molecular orbital of the irradiated material [17]. Over time, the electronic, vibrational, and rotational excitation of the molecules in the medium dissipates the excess kinetic energy of the electrons, resulting in a chemical change in polyaniline. This process enhances its conductivity and reduces its band gap energy by generating additional polarons [19]. Figure 7 illustrates the relationship between gamma dose and the absorption of the 800 nm band.

The disappearance of the signal at 800 nm below 20-kGy, as depicted in Figure 7, implies that the conductive form of PANI ES in ZnS/PANI core-shell is no longer present. This indicates that the polymerization process is governed by a specific dopant threshold. Furthermore, the polymer is not in the conductive form of PANI ES state since there's no significant shift in the 800 nm region of the UV-vis spectrum, which corresponds to the π ← π* transition of the benzenoid rings.

3.5. The Band Gap energy of ZnS/PANI Core-shell Nanocomposites

Optoelectronic components such as solar cells and LEDs experience significant advantages when incorporating ZnS/PANI in their manufacturing processes. Prior to delving into the discussion about the band structure and conduction band bottom potential of ZnS/PANI, it is essential to establish some fundamental concepts. The term "band structure" refers to the range of energy levels or bands accessible to electrons within a material. The lowest energy level within a material is situated at the bottom of the conduction band (CB), while the highest energy level occupied by electrons can be found at the top of the valence band (VB). The "bottom potential" of the conduction band represents the energy required to release an electron from the conduction band into a vacuum. In this context, the Standard Hydrogen Electrode (SHE) serves as the common reference electrode against which this energy is measured.

A method for determining the energy of the optical band gap in a semiconductor involves plotting the absorption coefficient α(v) as (α(v)hv)1/ m vs. hv versus the photon energy (hv), where "m" characterizes the nature of the transition. Various values of "m," including ½, 2, 3/2 or 3, correspond to different types of transitions, which can be either direct or indirect, permitted, prohibited, or partially

permitted. ZnS/PANI nanocomposites underwent examination to assess their band gap characteristics, revealing that the energy of the band gap decreases as gamma exposure increases. With the escalation of gamma radiation, a greater number of electrons are generated, signifying the development of a more conductive emeraldine salt (ES) type with a higher level of protonation. This phenomenon may offer an explanation for the observed behavior.

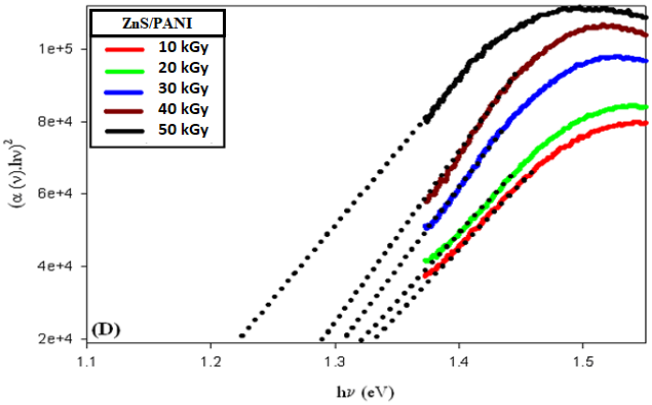


Fig. 7. Illustrates the energy difference between the bands in the ZnS/PANI core-shell structure.

Figure 7 presents graphs of $(\alpha(v)hv)^2$ *vs. hv* for different gamma irradiation levels, displaying ZnS/PANI nanocomposites dispersed in PVP. The direct band gap energy of PANI nanoparticles within PVP can be determined by extrapolating the data to $(\alpha(v)hv)^2 = 0$. However, as illustrated in Figure 7, the band gap energy (Eg) decreases with increasing irradiation dosage. This reduction in Eg can be attributed to the formation of more conductive PANI nanoparticles and an increase in polarons within the irradiated composite, both contributing to a smaller band gap energy for electronic π–π* transitions as the dose increases. Furthermore, as the protonation level of the PANI backbone rises, the optical band gap energy decreases from 1.34 to 1.22 *eV*. It's important to note that irradiation doping can induce various chemical changes in polymers, including cross-linking, chain scission, the creation of C=C bonds, production of alkyne groups, and depletion of heteroatoms (N, S, or O) [17].

We observed a decrease in the band gap energy from 1.34 to 1.22 eV as the radiation doses increased from 10 to 50 kGy, as shown in Figure 8. Irradiation of ZnS/PANI core-shell nanocomposites can lead to the breaking of hydrogen and hydroxyl groups in PANI and the formation of a carbonyl double bond (C=O), which may enhance the conductivity of PANI nanoparticles in ZnS/PANI core-shell nanocomposites. Moreover, understanding the mechanism of γ-ray interaction with the polymer can shed light on how ions, in the presence of DBSA, aid in the protonation processes that increase the conductivity of PANI nanoparticles and PANI [22, 23].

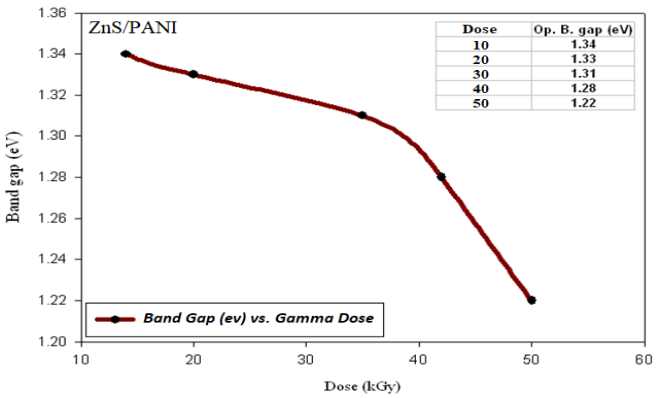


Fig. 8. A graph depicting the relationship between band gap energy and radiation doses (kGy) for the ZnS/Polyaniline structure.

Regarding ZnS/PANI, the band structure and conduction band (CB) bottom potential are influenced by several factors, including material composition, structure, and fabrication method. Previous research offers some general insights. For instance, a study published in the Materials Research Express (MRE) journal in 2020 investigated the band structure and electronic properties of ZnS/PVP nanocomposites. Utilizing first-principles calculations, the researchers predicted the electronic structure and optical properties of the material. Their findings suggested that the CB bottom potential of ZnS/PVP was approximately -3.7 eV relative to the standard hydrogen electrode (SHE), indicating its suitability for photocatalytic applications. Furthermore, the material exhibited a bandgap of approximately 3.6 eV, classifying it as a wide-bandgap semiconductor [17].

4. Conclusion

We conclude that the synthesis of PANI nanoparticles and the distribution of ZnS nanoparticles within PVP can be influenced by gamma-ray exposure. Moreover, gamma irradiation reduces the uniform dispersion of ions in the ZnS nanoparticles in the presence of aqueous electrons. Notably, in samples exposed to higher doses of gamma radiation, we observed an increased presence of ZnS nanoparticles coated with PANI. These results provide support for the proposed mechanisms we have detailed, thus confirming the attainment of our research objectives.

In the UV-visible absorption spectra of ZnS/PANI/PVP core-shell nanocomposites, the intensity of the broad absorption band around 800 nm, attributed to doped PANI in a bipolaronic state, grows as the PANI content in the composites increases. Examination by SEM and TEM demonstrates that the size of PANI nanoparticles decreases from over 400 nm at 10-kGy to approximately 10 nm at 50-kGy, with improved dispersion and no apparent influence from ZnS nanoparticles on the PANI morphology. This discovery provides evidence that ZnS nanoparticles serve as nucleation sites in the polymerization process, resulting in a continuous PANI coating. It was observed that spherical-shaped polyaniline nanocomposites (PANI) were doped with 18 wt% aniline and exposed to 50 kGy radiation dose.

An analysis of the morphology and UV-visible absorption data reveals that the interaction between ZnS and PANI occurs through three primary mechanisms: (a) π-π - stacking, (b) electrostatic interactions, and (c) hydrogen bonding. When polar groups, representing polymer charge carriers, interact with oxygenated groups, they can form ionic or coordinated complexes. The stability of the ZnS/PANI core-shell in PVP of the nanocomposites and the oxidation state of the doped ZnS/PANI is explained by the metal's interaction with the C-N and C=O functional groups in PANI/PVP. Transmission and scanning electron microscopy confirm the core-shell morphology of the nanocomposite ZnS quantum dots, comprising PANI nanoparticles with a thickness of approximately 10 nm surrounding a core with a mean particle size of about 5 nm.

Nanotechnology has emerged as a revolutionary force in the realm of solar cell materials, particularly in terms of enhancing cost-effectiveness. The integration of nanomaterials has opened up new avenues for improving the efficiency and overall performance of solar cells. One intriguing development in this field is the proposed use of ZnS/PANI nanocomposites. The combination of zinc sulfide and polyaniline in nanostructured form holds great promise for advancing the capabilities of solar cells. These nanocomposites have the potential to significantly impact both the power coefficient and overall efficiency of solar cells. The unique properties of ZnS/PANI nanocomposites, at the nanoscale level, contribute to improved light absorption, charge separation, and electron transport within the solar cell structure.

As we eagerly anticipate the results of the ongoing research and development involving ZnS/PANI nanocomposites, it is clear that such innovations have the potential to reshape the landscape of solar energy technology. The exploration of these advanced materials signifies a significant stride toward achieving sustainable and cost-effective energy solutions. The commendable efforts in developing and incorporating ZnS/PANI nanocomposites into solar cell materials deserve recognition for their potential to enhance the power coefficient and efficiency of solar cells. This work stands as a testament to the continual advancements in nanotechnology, bringing us closer to a future where clean and efficient energy sources are more accessible to a global audience.

These findings hold promise for applications in solar cell materials. The ZnS/PANI nanocomposite core-shell materials produced here will be valuable in future research on solar cell technology.

References

[1] B. B. Abdullah, S. Ali, B. Sertac, & A. Haitham, "Design and implementation of microcontroller based three phase induction motor experimental set," 10th International Conference on Smart Grid, June 27-29, 2022, Istanbul / Turkey.

[2] V. Matin, M. Ali, D. L. Donovin, F. E. John & M. I. Dan, "Coreless axial flux halbach array permanent magnet generator concept for direct-drive wind turbine," 13th International Conference on Renewable Energy Research and Applications, November 9 - November 13, 2024, Nagasaki, Japan.

[3] D. Nihat, U. Berat & B. Erdal, "Measurement and evaluation of solar panel data via DC power line," 10th International Conference on Smart Grid, June 27-29, 2022, Istanbul / Turkey.

[4] S. Satoshi & S. Orie, "Voltage control of DFIG-based wind turbine generator in rural grid," 13th International Conference on Renewable Energy Research and Applications, November 9 - November 13, 2024, Nagasaki, Japan.

[5] M. M. Shameem, S. Sasikanth, R. Annamalai & R. G. Raman, "A brief review on polymer nanocomposites and its applications," Materials Today 2021: Proceedings, vol. 45, pp. 2536–2539, DOI:10.1016/j.matpr.2020.11.254.

[6] F. R. Rangel-Olivares, E. M. Arce-Estrada & R. Cabrera-Sierra, "Synthesis and characterization of polyaniline-based polymer nanocomposites as anti-corrosion coatings," MDPI: Coatings 2021, 11(6), 653, DOI:10.3390/coatings11060653.

[7] R. Jabnoor, B. Manjunatha, M. AmbikaPrasad, A. Lagashetty, V. Basavarajappa & S. Kalyane, "Synthesis, characterisation and AC conductivity study of PANI/α-Fe2O3 nanocomposites," IOP Conference Series: Materials Science and Engineering, 2022, DOI:10.1088/1757-899X/1221/1/012001.

[8] S. S. Gasaymeh, S. Radiman, L. Y. Heng & E. Saion, "Gamma irradiation synthesis and influence the optical and thermal properties of cadmium sulfide (CdS)/poly (vinyl pyrolidone) nanocomposites," Am. J. Appl. Sci. 2010, 7 (4):500–8, DOI:10.3844/ajassp.2010.500.508.

[9] A. Kamal, M. Ashmawy, A. M. Algazzar & A. H. Elsheikh, "Fabrication techniques of polymeric nanocomposites: a comprehensive review," Proceedings of the Institution of Mechanical Engineers, Part C: Journal of Mechanical Engineering Science 2022, vol. 236, no. 9, pp. 4843–4861, DOI:10.1177/09544062211055662.

[10] M. M. Mahat, A. S. Sabere, J. Azizi & N. A. Amdan, "Potential applications of conducting polymers to reduce secondary bacterial infections among COVID-19 patients: a review. Emergent Materials," 2021, vol. 4, no. 1, pp. 279–292, DOI:10.1007/s42247-021-00188-4.

[11] D. A. Albuquerque, R. Ramos, C. E. Ireno, E. Martins, S. F. Durrant, & J. R. Bortoleto, "SnO2/ZnO heterostructure as an electron transport layer for perovskite solar cells," Materials Research, 2021, 24, 1–7, DOI:10.1590/1980-5373-MR-2021-0050.

[12] R. Zhang & H. Pang. "Application of graphene-metal/conductive polymer based composites in super capacitors," Journal of Energy Storage, 2021, vol. 33, DOI:10.1016/j.est.2020.102037.

[13] C. Idumah, E. Ezeani & I. Nwuzor, "A review: advancements in conductive polymers nanocomposites" Polymer-Plastics Technology and Materials, 2021, vol. 60, no. 7, pp. 756–783, DOI:10.1080/25740881.2020.1850783.

[14] S. S. Sambaza, A. Maity & K. Pillay, "Polyaniline-coated TiO2 Nanorods for photocatalytic degradation of bisphenol a in water," ACS Omega, 2020, 5, 29642–29656, DOI:10.1021/acsomega.0c00628.

[15] M. Rezvani, A. A. Asgharinezhad, H. Ebrahimzadeh & N. Shekari, " polyaniline-magnetite nanocomposite as an anion exchange sorbent for solid-phase extraction of chromium (VI) ions," Microchimica Acta, 2014, vol. 181, pp. 1887–1895, DOI:10.1007/s00604-014-1262-1.

[16] H. Virk & A. Srivastava, "Modification of optical, chemical and structural response of CR-39 polymer by 50 MeV lithium ion irradiation," Radiation Measurements, 2001, 34: 65–67, DOI:10.1016/S1350-4487(01)00122-6.

[17] S. S. Gasaymeh & A. N. Almansoori, "Novel formation mechanism of Ag/PANI/PVP core-shell nanocomposites," Results in Physics 2020, 16, DOI:10.1016/j.rinp.2019.102882.

[18] T. Prosa, M. Winokur, J. Moulton, P. Smith & A. Heeger, "X-ray diffraction studies of the three-dimensional structure within iodine-intercalated poly (3-octylthiophene)," Physical Review B, 1995, 51: 150-156, DOI:10.1103/physrevb.51.159.

[19] S. S. Gasaymeh, "Formation mechanism and characterization of PANI nanoparticles by hybrid chemical and gamma irradiation technique," American Journal of Applied Sciences 2018, 15 (12): 519.531, DOI:10.3844/ajassp.2018.519.531.

[20] T. Thanpitcha, A. Sirivat, A. M. Jamieson & R. Rujiravanit, "Preparation and characterization of polyaniline/chitosan blend film Carbohydrate," Polymers, 2006, 64: 560–568, DOI:10.1016/j.carbpol.2005.11.026.

[21] M. Wolszczak, J. Kroh & M. M. Abdel-Hamid, "Some aspects of the radiation processing of conducting polymers," Radiation Physics Chemistry, 1995, 45: 71-78, DOI:10.1016/0969-806X(94)E0025-E.

[22] N. Asima, M. H. Aminb, M.A. Alghoulc, M. Badieid, M. Mohammada, S. S. Gasaymeheh, N. Aminf & K. Sopian, "Key factors of desiccant-based cooling systems: materials," Applied Thermal Engineering. Volume 159, August 2019, 113946.

[23] M. Sakai & T. Takeshita, "Energy management system of electric motorcycles for power boost," 13th International Conference on Renewable Energy Research and Applications, November 9 - November 13, 2024, Nagasaki, Japan.